2005 International Linear Collider Workshop - Stanford, U.S.A.

Charge Asymmetries in $\gamma\gamma \to \mu^+\mu^- + \nu$'s / $\gamma\gamma \to W^\pm\mu^\mp + \nu$'s with Polarized Photons

D. A. Anipko, I. F. Ginzburg, K.A. Kanishev, A. V. Pak
Sobolev Institute of Mathematics and Novosibirsk State University, Novosibirsk, 630090, Russia
M. Cannoni, O. Panella
Istituto Nazionale di Fisica Nucleare, Sezione di Perugia, Via A. Pascoli, I-06123, Perugia, Italy

It is shown that the difference in the distributions of positive (μ^+, e^+) and negative charged leptons (μ^-, e^-) in reactions like $\gamma\gamma \to \mu^+\mu^- + \nu's$ and $\gamma\gamma \to W^\pm\mu^\mp + \nu's$ at $\sqrt{s} > 200$ GeV with polarized photons leads to observable *charge asymmetry* of muons which is sensitive to New Physics effects. The contribution of the process with intermediate τ-lepton in $\gamma\gamma \to W^\pm\mu^\mp + \nu's$ reaction is taken into account.

1. INTRODUCTION

The Photon Collider option of linear colliders [1] offers an the opportunity to study the physics of gauge bosons with sensitivity to effects coming from New Physics. It is expected that the charge asymmetry in the reactions here (*with neutral colliding particles*) will be a good tool for the discovery of New Physics effects. In this paper we study this effect in the Standard Model (SM) and make the first estimates of its sensitivity to the New Physics effects.

High energy photons will be produced at the Photon Colliders through Compton back-scattering of laser photons from high energy electron or (and) positron beams: they will not be monochromatic but will demonstrate an energy spectrum. The high energy part of this spectrum will mainly include photons with definite helicity $\lambda_i \approx \pm 1$ [2].

The SM cross section of $\gamma\gamma \to W^+W^-$ at center of mass energy greater than 200 GeV remains constant of about 80 pb up to higher energies and practically independent on photon polarization. At $\sqrt{s} > 200$ GeV this cross section is more than 10 times larger than the cross section of W production in e^+e^- mode, $\sigma_{e^+e^-\to W^+W^-}$. It will ensure very high event rate. The distribution of W-bosons in $\gamma\gamma \to W^+W^-$ process will be charge symmetrical but their polarization depends on polarization of initial photons. The distribution of muons in subsequent decay $W^\pm_\uparrow \to \mu^\pm\nu$ is asymmetrical due to CP conservation in the SM (see details in the end of Sect. 2).

The observable final state with two muons or $W + \mu$ with missing transverse momentum carried away by neutrinos can appear either via processes $\gamma\gamma \to \mu^+\mu^-\nu_\mu\bar{\nu}_\mu$ ($\gamma\gamma \to W\mu\nu$) or via cascade processes like $\gamma\gamma \to \tau^+\mu^-\nu_\tau\bar{\nu}_\mu$ ($\gamma\gamma \to W\tau\nu$) with subsequent $\tau \to \mu\nu_\mu\nu_\tau$ decay. The latter process enhances the total event rate (without cuts) by a value given by factor $B \equiv Br(\tau \to \mu\nu\nu) = 17\,\%$ for the $\gamma\gamma \to W\mu + \nu's$. Similar event rate enhancement in the process $\gamma\gamma \to \mu^+\mu^- + \nu's$ is $2B + B^2 \approx 37\,\%$.

The preliminary description of the simplest process $\gamma\gamma \to \mu^+\mu^-\nu_\mu\bar{\nu}_\mu$ has been done in ref. [5]. In the presented paper we consider this process in more details and taking into account the effects of the cascade process.

The accurate calculation of processes with 6 or more particles in the final state like $\gamma\gamma \to \mu^+\mu^-\nu_\mu\bar{\nu}_\mu\nu_\tau\bar{\nu}_\tau$ is a computationally challenging task with available software. Reasonable approximations made in the description of $\gamma\gamma \to \tau^+\mu^-\nu_\tau\bar{\nu}_\mu$ process provide high enough accuracy for our purposes.

Analyzing relative contributions of different diagrams to the process $\gamma\gamma \to \tau^+\mu^-\nu_\tau\bar{\nu}_\mu$, we have found that both total cross section and characteristics of asymmetry are described by the contribution of diagrams with intermediate double W-boson production (DRD diagrams, fig. 1(1)). Thus, to study the corrections to the main contributing process $\gamma\gamma \to \mu\mu\nu\nu$, we can limit ourselves with DRD diagrams and on-shell τ-lepton approximation. In this approximation polarization of τ in the rest frame of W is precisely known. With this knowledge the distribution of final muons from τ decay is given by convolution of calculated by CompHEP/CalcHEP distributions of τ-leptons with manually calculated distributions of muons in τ-decay (sec. 3.2).

• The analysis of the $\gamma\gamma \to W^{\pm}\mu^{\mp} + \nu's$ process allows us to see the main features of the studied effect – difference in the distributions of μ^+ and μ^- at given photon helicities, demanding less CPU time. The main part of the results is obtained for this process, assuming that W is detected as two jets or in some other way.

Most of our results are presented for *global asymmetry* – the difference in distributions of μ^+ and μ^- in the processes $\gamma\gamma \to W^{\pm}\mu^{\pm} + \nu$'s. *The correlative asymmetry* in μ^+ and μ^- momenta in each event can be more informative in the hunt for New Physics. We discuss it in sec. 4.

• We consider a collision of the photon with helicity λ_1 moving in the positive direction of z axis with a photon of helicity λ_2 moving in the opposite direction, this initial state is marked as $\gamma_{\lambda_1}\gamma_{\lambda_2}$ with $\lambda_i = \pm$ (left or right circular polarization). In particular, the initial state with $\lambda_1 = +1$, $\lambda_2 = -1$ is written as $\gamma_+\gamma_-$. With this choice of positive direction of z axis we define longitudinal momentum $p_{\parallel} \equiv p_z$ and transverse momentum $p_{\perp} \equiv \sqrt{p_x^2 + p_y^2}$. For definiteness, we present most of results for monochromatic photon beams at $\sqrt{s}_{\gamma\gamma} = 500$ GeV ($E_\gamma = 250$ GeV). In our calculations we anticipated the number of events as 10^6 per year and generate the same number of Monte-Carlo events.

Due to CP symmetry of the SM, differential cross-sections of the processes with the initial states $\gamma_+\gamma_+$ and $\gamma_+\gamma_-$ coincide with the those given the initial states $\gamma_-\gamma_-$ and $\gamma_-\gamma_+$, respectively, up to the exchange $\mu^+ \leftrightarrow \mu^-$. Moreover, the distributions of μ^- and μ^+ in the forward hemisphere for $\gamma_+\gamma_-$-case reproduce the distributions of μ^+ and μ^- in the backward hemisphere, respectively. (Some of these symmetries are seen in the presented plots, some were verified by separate calculation.) Therefore, in all cases the asymmetries Δ_L change signs in each hemisphere when the helicity changes to opposite. In particular, for the $\gamma_-\gamma_+$ collisions these asymmetries in forward and backward hemispheres have opposite signs. These symmetries break if any CP-violating interaction is essential.

• Our numerical results have been obtained with the CompHEP/CalcHEP packages [3], [4] in a version which allows to take into account the circular polarization of the initial photons [4].

• In our calculations we apply simultaneous cuts in escape angle θ of each observed particle and its transverse momentum $p_\perp$:

$$\begin{array}{rl} \pi - \theta_0 > \theta > \theta_0 & \text{with } \theta_0 = 10\ mrad, \\ p_\perp > p_{\perp 0} & \text{with } p_{\perp 0} = 10\ GeV. \end{array} \tag{1}$$

We apply additionally the same limitation in total transverse momentum for the sum of momenta of all observed particles. These simultaneous cuts allow to eliminate many backgrounds (since at $\sqrt{s} \le 1$ TeV charged particle(s) with missing transverse momentum $> p_{\perp 0}$ should have the escape angle $> 2p_{\perp 0}/\sqrt{s} > \theta_0$). The value of angular cut is chosen in correspondence with most optimistic anticipated ILC detector in TESLA version. We also study the influence of the $p_{\perp 0}$ cut on the effect.

2. DIAGRAMS, QUALITATIVE PICTURE. DRF APPROXIMATION

In SM at the tree level the process $\gamma\gamma \to \mu^+\mu^-\nu\bar{\nu}$ is described by 19 diagrams, which we subdivide at 5 types, shown in Fig. 1 (a similar classification was given also in Ref. [6]). The collection of diagrams within each type is obtained from the shown in figure with the exchange $+ \leftrightarrow -$, $\nu \leftrightarrow \bar{\nu}$ and permutations of photons. The process $\gamma\gamma \to W^+\mu^-\bar{\nu}$ is described by only first 3 groups of diagrams.

We supply the description of diagrams with analytical estimates of their contribution to the total cross section, based on the equations for $2 \to 2$ processes at $s \gg M_W^2$, with relation for SM gauge couplings $g^2 \sim g'^2 \sim \alpha$. The contribution from the interference with dominant DRD is roughly the same (with accuracy to sign), since DRD is large in only two regions of final phase space corresponding to W resonances while other contributions have no these peaks.

1. 3 double-resonant diagrams (DRD) of Fig. 1(1) describe WW pair production with subsequent decay. Corresponding contribution to the total cross section is $\sigma_d \sim (\alpha^2/M_W^2) Br^2(W \to \mu\nu)$.
2. 4 single-resonant diagrams (SRD) of Fig. 1(2) with W exchange in t–channel contribute to the total cross section $\sigma_{sW} \sim (\alpha^3/M_W^2) Br(W \to \mu\nu) \sim \sigma_d \alpha / Br(W \to \mu\nu)$.

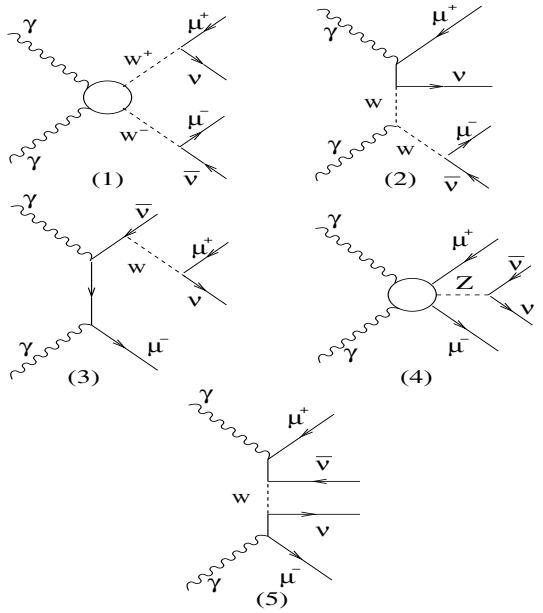

Figure 1: The types of tree level Feynman diagrams contributing to $\gamma\gamma \to \mu^+\mu^-\nu\bar{\nu}$.

3. 4 single resonant diagrams with ν exchange in t–channel (gauge boson bremsstrahlung), Fig. 1(3). The contribution to the total cross section is $\sigma_{s\mu} \sim (\alpha^3/s)Br(W \to \mu\nu) \sim \sigma_d \alpha/Br(W \to \mu\nu)(M_W^2/s)$.
4. 6 diagrams with radiation of Z boson in the process $\gamma\gamma \to \mu^+\mu^-$, Fig. 1(4) give asymptotic contribution $\sigma_Z \sim (\alpha^3/s)Br(Z \to \nu\bar{\nu})$.
5. 2 multi-peripheral non-resonant diagrams Fig. 1(5) with $\sigma_n \sim \alpha^4/M_W^2$.

These estimates show that at the considered energies all contributions to the cross section are negligible in comparison with that of DRD (at the level of radiative corrections) except for SRD contribution. Our numerical analyses support this conclusion. It turned out that for $\gamma\gamma \to W\mu\nu$ the SRD contribution itself is about 5 % from that of DRD and the interference of this contribution with DRD is destructive so that the DRD contribution differs from total cross section by approximately 1.3 % for $\gamma_\pm\gamma_\pm$ collision and 0.6 % for $\gamma_\pm\gamma_\mp$ collision (for the process $\gamma\gamma \to \mu^+\mu^- + \nu's$ these inaccuracies are twice as large). This fact allows us to use **DRD approximation** to describe corrections from the cascade processes (i.e. include only DRD diagrams). In sec. 3.4 we show that the DRD approximation describes the contribution from cascade processes to the observable charge asymmetries with high enough accuracy.

• **Qualitative picture**. Our numerical studies support with high precision the qualitative picture of asymmetry, expected in DRD approximation.
(*i*) At $\sqrt{s} > 200$ GeV the $\gamma\gamma \to W^+W^-$ cross section practically doesn't depend on photon polarizations.
(*ii*) In the $\gamma\gamma \to W^+W^-$ process W's are distributed mainly around the forward and backward directions with average transverse momentum $\sim M_W$ (distribution $\propto 1/(p_\perp^2 + M_W^2)^2$ [7]).
(*iii*) In this process we have an approximate helicity conservation (see helicity amplitudes in [8]). The helicity of $W^\pm$ moving in the positive direction of z axis $\lambda_{W1} \approx \lambda_1$, while $\lambda_{W2} \approx \lambda_2$, is independent on the charge sign of W.
(*iv*) Let z'–axis be directed along W three–momentum and $\varepsilon \approx M_W/2$ and $p_{z'}$ be energy and longitudinal momentum of μ in the W rest frame. It is easy to calculate that the distribution of muons from the decay of W with charge $e = \pm 1$ and helicity $\lambda = \pm 1$ in its rest frame is $\propto (\varepsilon - e\lambda p_{z'})^2$ (the transverse momenta of muons are distributed roughly isotropically relative to W momentum within the interval $p_\perp < m_W/2$). In other words, the distribution of muons from $W^\pm$ decay has a peak along W momentum at $e\lambda_W = -1$ and opposite to W momentum at $e\lambda_W = +1$. These distributions are boosted to the distributions in the $\gamma\gamma$ collision frame. For example for collision of photons in $\gamma_-\gamma_-$ initial state, produced μ^- are distributed around the upper value of their longitudinal momentum (in forward

and backward direction), while produced μ^+ are concentrated near the zero value of their longitudinal momentum. Simultaneously, the same boost makes the distribution in $p_\perp$ wider in the first case and narrower in the second case.

3. GLOBAL ASYMMETRY

In this section we present results of numerical calculation of *the global asymmetry*, which is the difference in distributions of μ^+ and μ^- in the processes $\gamma\gamma \to W^+\mu^- + \nu$'s and $\gamma\gamma \to W^-\mu^+ + \nu$'s. For these problems we consider the normalized mean values of longitudinal $p_\parallel^\mp$ and transverse $p_\perp^\mp$ momenta of μ^- or μ^+, for definiteness – for the events when the longitudinal momentum of μ is in the forward hemisphere ($p_\parallel > 0$), and take their relative difference as a measure of the longitudinal Δ_L and transverse Δ_T charge asymmetry:

$$P_L^\pm = \frac{\int p_\parallel^\pm d\sigma}{E_{\gamma max}\int d\sigma}\,, \quad P_T^\pm = \frac{\int p_\perp^\pm d\sigma}{E_{\gamma max}\int d\sigma}\,,$$
$$\Delta_L = \frac{P_{L+}^- - P_{L+}^+}{P_{L+}^- + P_{L+}^+}\,, \quad \Delta_T = \frac{P_{T+}^- - P_{T+}^+}{P_{T+}^- + P_{T+}^+}\,. \tag{2}$$

(These definitions are useful for non-monochromatic case as well.)

3.1. Main process $\gamma\gamma \to W\mu\nu$

We start with the study of asymmetry neglecting the cascade channel.

• First, we present plots for the distributions of muons in the $p_\parallel$, $p_\perp$ plane, $\partial^2\sigma/(\partial p_\parallel \partial p_\perp)$ at different photon polarizations, Figs. 2.

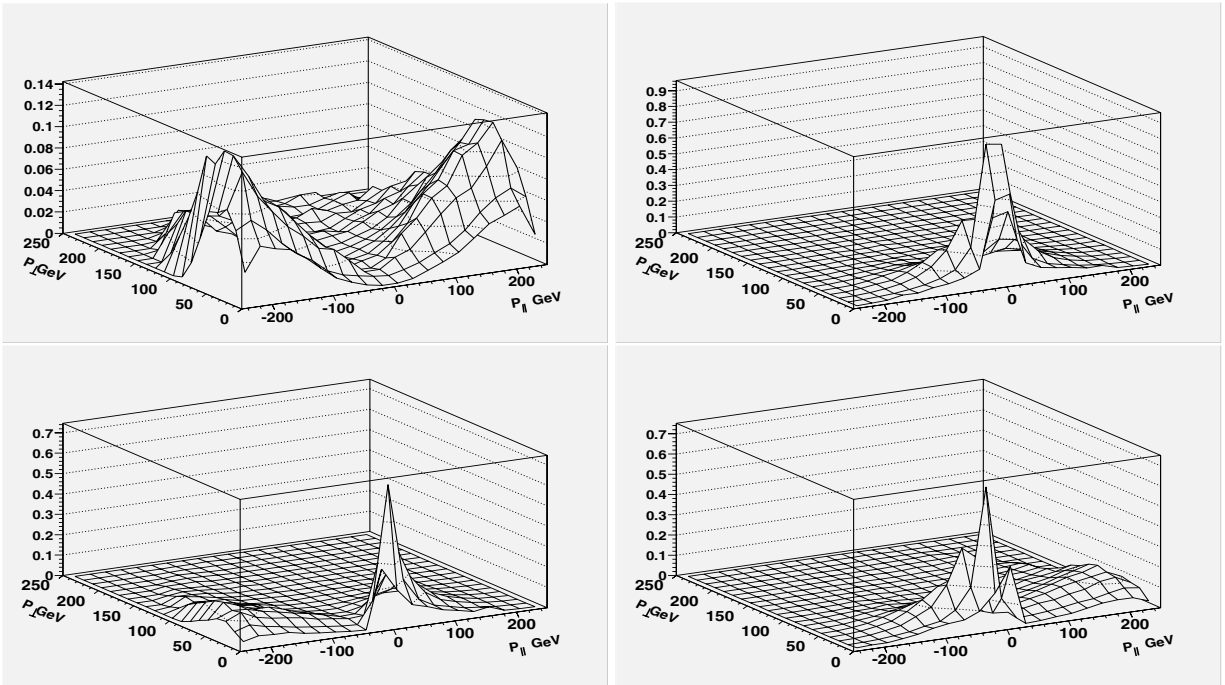

Figure 2: Muon distribution in in $\gamma_-\gamma_- \to W\mu\nu$ (upper plots) and in $\gamma_+\gamma_- \to W\mu\nu$ (lower plots), left – μ^-,right – μ^+

Presented figures show explicitly strong difference in the distributions of negative and positive muons just as strong dependence of distributions on photon polarizations. These figures clearly show that the charge asymmetry in the process is **a strong effect**.

• To obtain more definite quantitative description, we have calculated asymmetry quantities (2) for these very photon polarizations.

The Monte Carlo calculations simulate experiment and have statistical uncertainty similar to that in the future experiment. The value of such uncertainty for the integral characteristics like (2) cannot be predicted from general reasons. We find it useful to obtain this statistical uncertainty of considered quantities at given expected number of events (about 10^6). For this goal we repeated our calculation 5 times with different random number inputs for Monte Carlo generator (with CalcHEP [4]) and consider as an independent set of observations data obtained simultaneous change λ_1, $\lambda_2 \to -\lambda_1$, $-\lambda_2$, $\mu^- \leftrightarrow \mu^+$ (this change should not change distributions due to CP conservation in SM). Certainly, this uncertainty changes with variation of applied cuts. We present all quantities for the values (1).

Table I presents obtained mean momenta for the positive and negative muons and corresponding asymmetry quantities together with their statistical uncertainties. Here the parameter N takes values N=L (longitudinal) and N=T (transverse). Everywhere under the value of each considered quantity we present its statistical uncertainty in percents.

One can see that the values of asymmetry are typically 20-50%. That is *a huge and easily observable effect.* Statistical uncertainty is at the level of radiative corrections, so our tree-level approximation is sufficient for the description of the future experiments.

We checked that with the change of sign of both photon helicities mean muon momenta for negative and positive muons change their places (within statistical accuracy) so that the the quantities $\Delta_{L,T}$ change their sign with this change of polarization.

Note that the scale of longitudinal distributions is given by initial photon energy while the scale for transverse distributions is given by W mass. Thus, mean transverse momenta are usually smaller than longitudinal.

Table I. *Charge asymmetry quantities and their statistical uncertainties for $\gamma_{\lambda_1}\gamma_{\lambda_2} \to W\mu\nu$ process.*

$\gamma_{\lambda_1}\gamma_{\lambda_2}$	N	P_N^- δP_N^-	P_N^+ δP_N^+	Δ_N $\delta\Delta_N$
$\gamma_-\gamma_-$	L	0.599 0.35%	0.170 0.37%	0.557 0.37%
	T	0.338 0.96%	0.150 0.42%	0.386 0.99%
$\gamma_+\gamma_-$	L	0.209 0.82%	0.556 0.34%	-0.454 0.52%
	T	0.159 0.72%	0.249 0.82%	-0.220 2.52%

3.2. Cascade process contribution, $\gamma\gamma \to W\tau\nu \to W\mu\nu\nu\nu$

In the frame of DRD approximation the polarization of τ in the rest frame of W is given by SM vertex, $\tau^+ W_\mu^- \gamma^\mu(1-\gamma^5)\nu_\tau + h.c.$. Due to $\gamma^\mu(1-\gamma^5)$ factor, τ helicity coincides with that of ν_τ, it is positive for τ^+ and negative for τ^- (with accuracy to m_τ/M_W). For each generated event momenta of all particles are known. The spin vector of τ is expressed easily via momenta of τ and ν_τ, p and p_ν respectively, as

$$\pm s/2, \quad \text{where} \quad s = \frac{1}{\sqrt{2}}\left(\frac{p_\nu m_\tau}{(pp_\nu)} - \frac{p}{m_\tau}\right) \qquad \begin{cases} + & \text{for } \tau^+, \\ - & \text{for } \tau^-. \end{cases} \tag{3}$$

Note that the quantity $2pp_\nu = M_W^2 - m_\tau^2 + \mathcal{O}\left(-_{\mathcal{W}}\mathcal{M}_{\mathcal{W}}\right)$.

Denoting the momentum of μ by k, the distribution of muons in τ-decay with momentum p and spin $\pm s$ can be written neglecting muon mass as

$$f = \frac{4}{\pi E_\tau m_\tau^4}\left[(3m_\tau^2 - 4pk)pk + ks\cdot m_\tau(4pk - m_\tau^2)\right] d\Gamma, \quad , \tag{4}$$

where $d\Gamma$ isa phase space element boosted to the lab frame. In the τ rest frame $d\Gamma = \theta\left(m_\tau/2 - k\right) d^3k/E_\mu$.

The distribution of final muons from τ decay is given by convolution of calculated precisely in tree approximation by CompHEP/CalcHEP distributions of τ-leptons, with distribution (4). The essential feature of this convolution is the fact that the decay $\tau \to \mu\nu_\tau\nu_\mu$ involves three particles (unlike discussed above $W \to \mu\nu_\mu$ decay). Here the effective mass of the neutrino pair $m_{\nu\nu}$ varies from 0 to almost m_τ. Therefore, the corresponding μ distribution is usually contracted as compared to τ distribution when we boost it to the collision frame ($E_\mu \le E_\tau(1 - m_{\nu\nu}^2/m_\tau^2)$). Therefore, the distribution of muons in the cascade process is similar in the main features to that of incident τ,

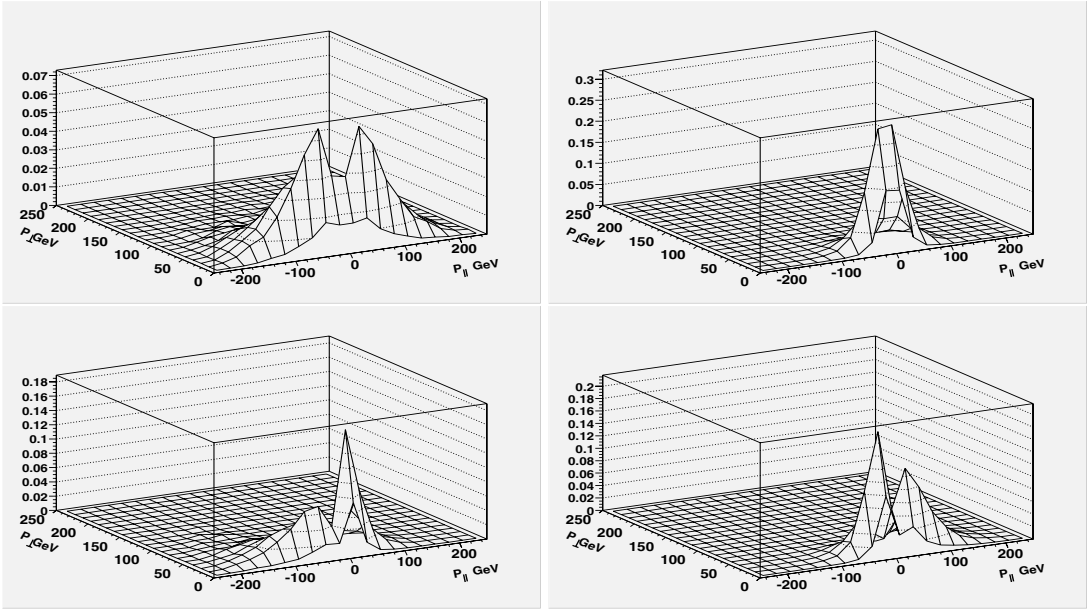

Figure 3: *Muon distribution in* $\gamma_-\gamma_- \to W\mu\nu\nu\nu$ *(upper plot) and in* $\gamma_+\gamma_- \to W\mu\nu\nu\nu$ *(lower plot), left –* μ^-*,right –* μ^+

discussed above, but it is strongly contracted to the point of origin. It is illustrated by Figs. 3 in their comparison with Figs. 2.

Since these distributions are concentrated at small $p_\parallel$, $p_\perp$ the cuts (1) reduce this contribution much stronger than the main contribution. It also reduces the inaccuracy in the final asymmetry introduced by DRD approximation.

- **Resulting asymmetries.**

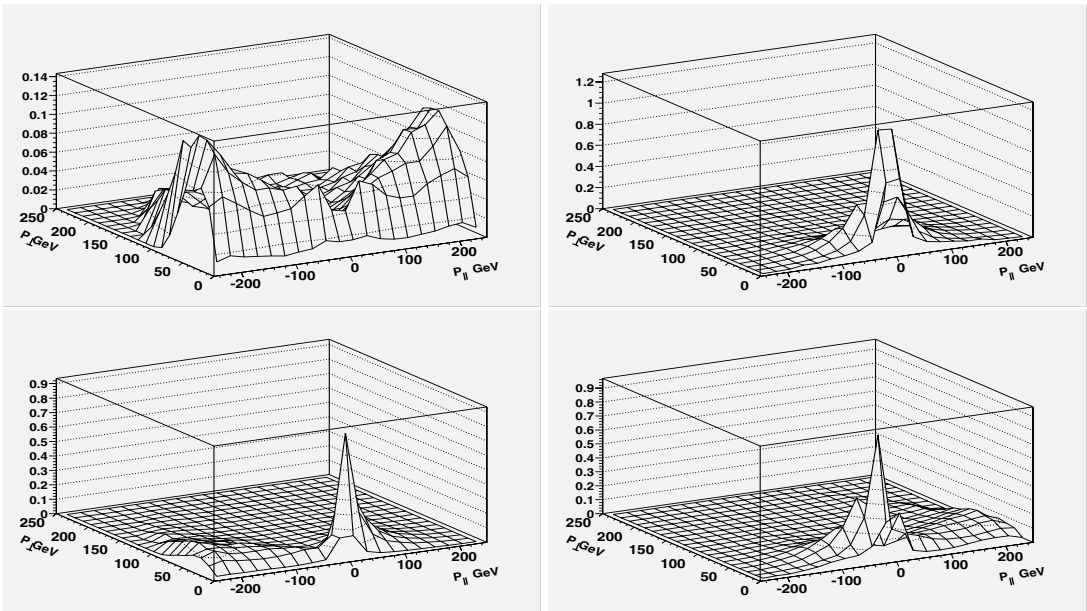

Figure 4: *Total muon distribution in* $\gamma_-\gamma_- \to W\mu + \nu's$ *(upper plot) and* $\gamma_+\gamma_- \to W\mu + \nu's9$*lower plot), left –* μ^-*,right –* μ^+

Figures 4 show the total observable distributions of muons — the sum of distributions of muons in $\gamma\gamma \to W\mu\nu$ and $\gamma\gamma \to W\tau\nu \to W\mu\nu\nu\nu$ and the table II represents the corresponding total asymmetry quantities for $p_{\perp 0} = 10$ GeV. The comparison with fig. 2 and Table I shows that taking into account the cascade process changes form of distribution of muons at only small momenta and the asymmetry parameters $\Delta_{L,T}$ decrease due to cascade process in average by about 3 % only.

Table II. *Resulting asymmetry quantities.*

$\gamma_{\lambda_1}\gamma_{\lambda_2}$	N	P_N^-	P_N^+	Δ_N
$\gamma_-\gamma_-$	L	0.548	0.164	0.539
	T	0.311	0.142	0.374
$\gamma_+\gamma_-$	L	0.199	0.513	-0.440
	T	0.152	0.232	-0.207

3.3. Dependence on $p_\perp$ cut

It is natural to expect that New Physics effects will be switched on at the relatively large transverse momenta. That is why we study the dependence of observed effects on the cut value $p_{\perp 0}$ (1) – see fig. 5.

The left plot here represents the dependence of the total cross-section on $p_{\perp 0}$. Naturally, it decreases with growth of $p_{\perp 0}$ (full line in the figure, right scale – fraction of total cross section corresponding this cut). The relative value of

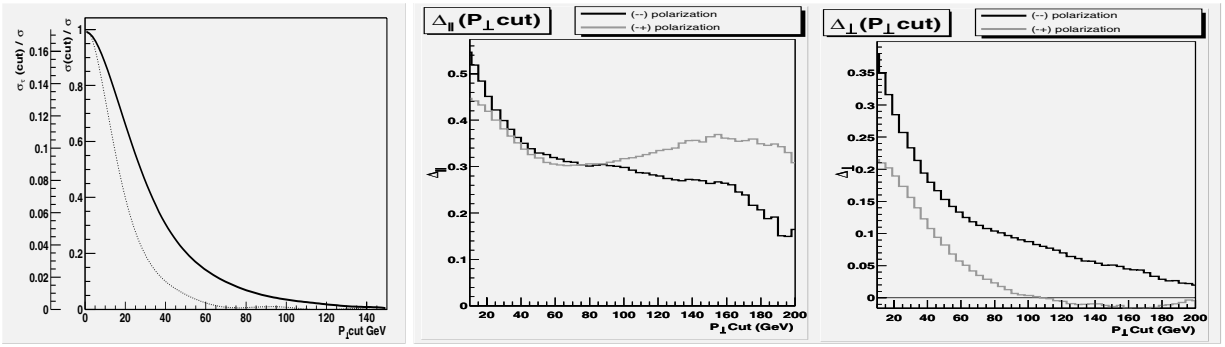

Figure 5: The $p_{\perp 0}$ dependence of cross section and asymmetry.
Left plot – cross section. Full line, right scale – fraction of σ_{tot} truncated by cut, dotted line, left scale – fraction of cascade process in the total truncated cross section. Cental plot – Δ_L, right plot – Δ_T, full lines – for $\gamma_-\gamma_-$, dotted lines – for $\gamma_-\gamma_+$

the contribution of process with intermediate τ (dotted line, left scale – relative fraction of cascade process) decreases much faster that total cross section. It is caused by contraction of phase space for muons obtained from decay of τ, discussed in sec. 3.2.

The central and right plots in fig. 5 show the dependence of asymmetries $\Delta_\perp$ and $\Delta_\parallel$ on $p_{\perp 0}$. We see that longitudinal charge asymmetry remains large even with large cuts while transverse charge asymmetry diminishes with $p_{\perp 0}$ growth.

3.4. Quality of DRD approximation

The resulting distributions include the complete tree-level results of $\gamma\gamma \to W\mu\nu$ and DRD approximation for cascade contribution. The inaccuracy implemented by this approximation is given by product

$$\delta_{approx}(p_{\perp 0}) = \delta\sigma_\tau(p_{\perp 0}) \times \delta_{DRD}(p_{\perp 0})\,. \qquad (5)$$

Here the first factor is a fraction of total cross section of cascade process (fig. 5, left) and the second factor is inaccuracy of DRD approximation for given physical quantity (asymmetry parameters $\Delta_{L,T}$ (2)). We determine this inaccuracy by comparison of exact calculation for the process $\gamma\gamma \to W\tau\nu$ with its calculation in DRD approximation. These inaccuracies for different values of $p_{\perp 0}$

Table III. *Inaccuracy of DRD approximation for $\Delta_{L,T}$ at different $p_{\perp 0}$.*

$p_{\perp 0}$, GeV		10	40	80	120
$\gamma_-\gamma_-$	$\delta\Delta_L$,%	0.9	1.5	1.1	5.7
	$\delta\Delta_T$,%	2.3	3.6	5.7	5.3
$\gamma_+\gamma_-$	$\delta\Delta_L$,%	0.7	2.1	4.1	4.4
	$\delta\Delta_T$,%	3.45	4.1	7.4	31

are presented in the Table III.

One can see that the inaccuracy of DRD approximation in average increases slowly with the growth of $p_{\perp 0}$. This inaccuracy is larger for the transverse asymmetry, than for the transverse one.

The extremely large inaccuracy $\delta\Delta_T = 31$ % at $p_{\perp 0}$ appears only in the case when cascade contribution to the result is negligible (see fig. 5, left) and the asymmetry itself also practically disappears (see fig. 5, right, dotted line).

For $p_{\perp 0} = 10$ GeV the first factor in the estimate (5) is about 0.13. With the second factor given in the Table III one can see that the obtained inaccuracy is lower than the statistical uncertainty in the cross section (Table I).

With the growth of $p_{\perp 0}$ the first factor decreases fast (fig. 5, left) while the second factors increases slowly (Table III). Therefore, the DRD approximation has a good precision for the description of cascade contribution in summary distribution.

4. CORRELATIVE ASYMMETRIES

Correlative asymmetry is an asymmetry in μ^+ and μ^- momenta in each event, averaged over events in the process $\gamma\gamma \to \mu^+\mu^- + \nu's$ where both muons are recorded. This asymmetry can be in principle more sensitive to the delicate effects of New Physics however it will be based on the lower counting rate. The corresponding kinematical variables are introduced in sect.

The first problem here is to find some representative variables in the 5–dimensional $(\vec{p}_+, \vec{p}_-)$ phase space. For this purpose we consider the monochromatic $\gamma\gamma \to \mu^+\mu^-\nu\bar{\nu}$ process. In this respect we study various "natural" dimensionless variables.

$$v = \frac{4(p_{\perp +}^2 - p_{\perp -}^2)}{M_W^2}, \quad u = \frac{4(p_{\parallel +}^2 - p_{\parallel -}^2)}{M_W^2}, \quad vvn = \frac{4(p_{\parallel +}\epsilon_+ - p_{\parallel -}\epsilon_-)}{M_W^2}. \tag{6}$$

For the $\gamma_-\gamma_-$ and $\gamma_+\gamma_+$ collisions the distributions in the forward and backward hemispheres are identical. Therefore, in this case the variables u and v are useful while vvn can not be useful. Vice versa, for the $\gamma_-\gamma_+$ collision the variable vvn is useful while u and v are not. The distributions in these variables are shown in fig. 6.

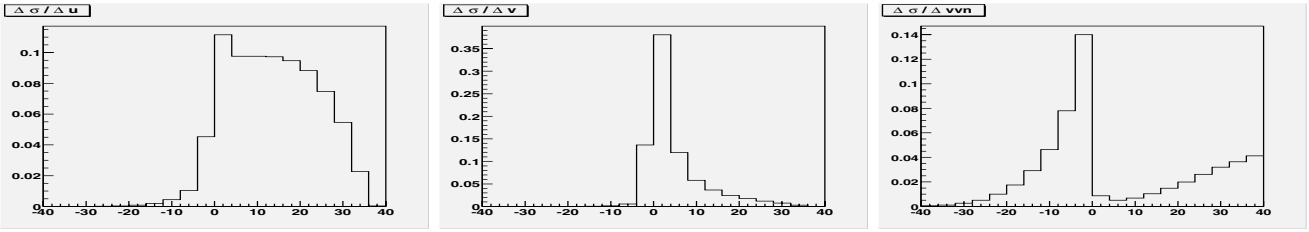

Figure 6: Distribution in u (left) and v (center) for $\gamma_-\gamma_-$ collision. Right: Distribution in vvn for $\gamma_-\gamma_+$ collision.

5. DISCUSSION AND OUTLOOK

• The effects considered so far are identical for electrons and muons. So that, absolutely the same asymmetry will be observed in $e^+\,e^-$, $e^+\,\mu^-$, $\mu^+\,e^-$ distributions. All these contributions should be added for a complete analysis. This will enhance the value of the cross section for $\gamma\gamma \to \mu^+\mu^-\nu\bar{\nu}$ from 1.2 to 4.8 pb and for $\gamma\gamma \to W^+\mu^-\bar{\nu}$, etc. to 30 pb (millions of events per year). (Here cascade processes like $\gamma\gamma \to W\tau\nu \to W\mu\nu\nu\nu$ are taken into account.)

• The real photon collision at Photon Colliders will be not monochromatic [2]. At the first glance, the influence of "realistic" photon energy spectra will smooth discussed asymmetries. First estimates of this phenomenon performed in ref. [5] showed that this non-monochromaticity decreases the considered asymmetries only weakly.

• We plan to consider such a charge asymmetry for discovery of New Physics effects, in particular, in case of existence of some new particles and interactions (e.g. MSSM). The choice of useful variables and suitable parameter range for better sensitivity to New Physics effects will be a natural counterpart of this activity. The first estimates of the potential in these studies were made in ref. [5]. It was shown there that the the charge asymmetry is sensitive to the quadruple momentum of W and less sensitive to its anomalous magnetic moment. Besides, the charge asymmetry appears to be sensitive to the production of new heavy particles.

Acknowledgments

This work is supported by grants RFBR 05-02-16211, NSh-2339.2003.2 and by the European Union under contract N. HPMF-CT-2000-00752.

References

[1] B. Badelek *et al. Int. J. Mod. Phys.* **A 19** (2004) 5097-5186
[2] I. F. Ginzburg, G. L. Kotkin, V. G. Serbo and V. I. Telnov, Nucl. Instrum. Meth. 205 (1983) 47;
I. F. Ginzburg, G. L. Kotkin, S. L. Panfil, V. G. Serbo and V. I. Telnov, Nucl. Instrum. Meth. A 219 (1984) 5.
[3] E. Boos et al. Nucl. Instr. Meth. **A534** (2004) 250; hep-ph/0403113
[4] A. Pukhov, hep-ph/0412191
[5] D. A. Anipko, M. Cannoni, I. F. Ginzburg, A. V. Pak, O.Panella, *Nucl. Phys.* **B** *Proc. Suppl.* **126** (2004) 354–359; hep-ph/0306138; hep-ph/0410123.
[6] E. Boos and T. Ohl, Phys. Lett. B 407 (1997) 161, hep-ph/9705374.
[7] I.F. Ginzburg, G.L. Kotkin, S.L. Panfil, V.G. Serbo, Nucl. Phys. B 228 (1983) 285.
[8] M.Baillargeon, G. Belanger, F. Boudjema. hep-ph/9405359
[9] I.F. Ginzburg, G.L. Kotkin, Eur. Phys. J. C 13 (2000) 295.
[10] K. Hagiwara et al., Phys. Rev. D 66, 010001 (2002)